SOLVING THREE-DIMENSIONAL NAVIER-STOKES FLOWS USING FINITE ELEMENTS METHOD

Fernanda Paula Barbosa, ferpaula@icmc.usp.br
USP - ICMC - Institute of Mathematical Science and Computation
Department of Applied Mathematics and Statistics - Sao Carlos, SP - Brazil

Norberto Mangiavacchi, norberto.mangiavacchi@gmail.com
UERJ - Department of Mechanical Engeneering - Rio de Janeiro, RJ - Brazil

Antonio Castelo Filho, castelo@icmc.usp.br
USP - ICMC - Institute of Mathematical Science and Computation
Department of Applied Mathematics and Statistics - Sao Carlos, SP - Brazil

Abstract. *This paper presents the development of a numerical method for the simulation of incompressible fluid flow over a three-dimensional domain, where the Navier-Stokes equations were written under an Eulerian formulation and discretized by the Finite Elements Method. The semi-Lagrangian method was used to discretize the convective terms and the components of velocity and pressure were decoupled through the use of a method based on LU decomposition. The three-dimensional domain was represented by a mesh, represented by a topological data structure, formed with cells forming linear wedge elements. Experiments solving the well known problem of backward-step were made in order to analyse the consistency of the proposed method on theoretical basis. The results showed a good approximation and pointed out the stability of the proposed method.*

Keywords: *Numerical Simulation, Navier-Stokes Equation, Fluid Mechanics, Finite Elements Method*

1. INTRODUCTION

In the study of incompressible fluid flows, the mathematical modeling of the conservation laws is well stated by Navier–Stokes equations and the mass conservation equations. The numerical simulation of fluid flow over many applications requires the use of numerical techniques of high efficiency, demanding high computational power. The need for numerical simulation in CFD is justified by the lack of analytical solutions of the Navier-Stokes equations for most practical cases.

A numerical simulation can be seen as a relation between theoretical and practical results, being a new solution to certain problems, attracting attention of many researchers. In order to apply the numerical solution to a problem, mathematical expressions must be derived. Such expressions are usually defined from the application of physical principles, described by laws and principles suitable to the phenomenon, such as mass conservation, energy and movement (Anderson, 1995)(Batchelor, 1970)(Fortuna, 2000) (Maliska, 1995)(Panton, 1984)(Peyret and Taylor, 1983)(Flecther, 1992) (Ferziger and Períc, 1999).

In this paper, a numerical model is proposed for the solution of three dimensional Navier–Stokes equations (momentum and mass conservation equations). The finite elements method (Zienkiewicz, 2000)(Becker et al., 1981)(Zienkiewicz and Cheung, 1965)(Chung, 1978) is used for the discretization of the proposed problem, where the Galerkin method is used for the spatial discretization and the semi-lagrangean method is used for the discretization of the material derivative. The latter derivative includes the convective term, responsible for the non linearity of the problem.

2. FORMULATION

The governing equations are the non-dimensional mass and momentum equations in conservative form where in three-dimensional coordinates can be written as

$$\frac{D(\rho\mathbf{u})}{Dt} = -\nabla p + \frac{1}{Re}\nabla\cdot[\mu(\nabla\mathbf{u}+\nabla\mathbf{u}^T)] + \frac{1}{Fr^2}\rho\mathbf{g} \tag{1}$$

and the equation of continuity

$$\nabla\cdot\mathbf{u} = 0. \tag{2}$$

where $Re = (LU)/\nu$ and $Fr = U/(\sqrt{gL})$ are the non-dimensional Reynolds and Froude numbers, respectively. Hence, L and U are the length and velocity scales, respectively, ν is the kinematic viscosity, and g denotes the gravitational constant, $g = |\mathbf{g}| = |(g_x, g_y, g_z)|$. Furthermore, $\mathbf{u} = (u, v, w)^t$ is the velocity vector while p is the non-dimensional pressure.

3. DISCRETIZATION

The three-dimensional domain is represented by a mesh, manipulated by a topologic data structure, formed with cells defining linear wedge elements. The shape functions interpolating the discrete approximations are assumed to be linear, and each node of the mesh has four degrees of freedom for the velocity and pressure properties.

3.1 Variational Formulation

Considering the Navier–Stokes equations for incompressible flows, written in the eulerian formulation expressed in the non-dimensional form as

$$\frac{D(\rho\mathbf{u})}{Dt} + \nabla p - \frac{1}{Re}\nabla \cdot \left[\mu\left(\nabla\mathbf{u} + \nabla\mathbf{u}^{\mathbf{T}}\right)\right] - \frac{1}{Fr^2}\rho\mathbf{g} = 0 \tag{3}$$

$$\nabla \cdot \mathbf{u} = 0 \tag{4}$$

valid on a domain $\Omega \subset \mathbb{R}^m$ under the boundary conditions

$$\mathbf{u} = \mathbf{u}_\Gamma, \text{ em } \Gamma_1 \tag{5}$$

$$u_t = 0 \text{ e } \sigma^{\text{nn}} = 0, \text{ em } \Gamma_2. \tag{6}$$

Consider the subspace

$$\mathbb{V} = H^1(\Omega)^m = \left\{\mathbf{v} = (v_1, \dots, v_m) : v_i \in H^1(\Omega), \forall i = 1, \dots, m\right\} \tag{7}$$

where $H^1(\Omega)$ is the *Sobolev* space given by

$$H^1(\Omega) = \left\{v \in L^2(\Omega) : \frac{\partial v}{\partial x_i} \in L^2(\Omega), i = 1, \dots, m\right\} \tag{8}$$

with $L^2(\Omega)$ being a infinity dimension space defined as

$$L^2(\Omega) = \left\{v : \Omega \rightarrow \mathbb{R}, \int_\Omega v^2 d\Omega < \infty\right\} \tag{9}$$

And $\mathbb{V} = H^1(\Omega)^m$ is the cartesian product of m spaces $H^1(\Omega)$.

Defining

$$\mathbb{V}_{\mathbf{u}\Gamma} = \mathbf{v} \in \mathbb{V} : \mathbf{v} = \mathbf{u}_\Gamma \text{ in } \Gamma_1, \ \mathbb{V}_0 = \mathbf{v} \in \mathbb{V} : \mathbf{v} = \mathbf{0} \text{ in } \Gamma_1 \tag{10}$$

$$\mathbb{P}_{p\Gamma} = q \in L^2(\Omega) : q = p_\Gamma \text{ in } \Gamma_2 \tag{11}$$

the weak formulation of the problem can be written as: find $\mathbf{u}(\mathbf{x}, t) \in \mathbb{V}_{\mathbf{u}\Gamma}$ e $p(\mathbf{x}, t) \in \mathbb{P}_{p\Gamma}$ such that

$$\int_\Omega \frac{D(\rho\mathbf{u})}{Dt} \cdot \mathbf{w} d\Omega - \int_\Omega \nabla p \cdot \mathbf{w} d\Omega - \int_\Omega \frac{1}{Re}\nabla \cdot \left[\mu\left(\nabla\mathbf{u} + \nabla\mathbf{u}^T\right)\right] : \mathbf{w} d\Omega - \int_\Omega \frac{1}{Fr^2}\rho\mathbf{g} \cdot \mathbf{w} d\Omega = 0.$$

$$\int_\Omega (\nabla \cdot \mathbf{u})\, q d\Omega = 0 \tag{12}$$

for all $\mathbf{w} \in \mathbb{V}_0$ e $q \in \mathbb{P}_{p\Gamma}$.

The discretization of (12) is made by using linear shape functions and Galerkin weighting functions. Integrating over the wedge elements results in an ODE system, which is solved using the projection method described as follows. The time derivatives are integrated by an implicit scheme. As in the Lagrangian formulation the non-linear terms do not appear, the matrices are defined symmetric positive and thus the conjugate gradient method can be applied to solve the linear systems.

3.2 Galerkin's Method

After the variational formulation of the governing equations, the approximation phase takes place using the Galerkin's method. Consider the governing equations in its non-dimensional and variational form (Eq. 12) and letting NV be the number of velocity points, NP the number of pressure points and NE the number of finite elements of the mesh that discretizes the domain Ω. The Galerkin's method consists on replacing the following terms on Eq. (12):

$$u(\mathbf{x},t) \approx \sum_{n=1}^{NV} \psi_n(\mathbf{x}) u_n(t), \qquad v(\mathbf{x},t) \approx \sum_{n=1}^{NV} \psi_n(\mathbf{x}) v_n(t) \tag{13}$$

$$w(\mathbf{x},t) \approx \sum_{n=1}^{NV} \psi_n(\mathbf{x}) w_n(t), \qquad p(\mathbf{x},t) \approx \sum_{n=1}^{NP} P_n(\mathbf{x}) p_n(t) \tag{14}$$

that are semi-continuous approximations, that is, continuous in time (t) and discrete in space (x). Here, $\psi_n(x)$ represent the interpolation functions used for the velocity and $P_n(x)$ the interpolating functions for the pressure.

The momentum equation is normally evaluated in all the free nodes of velocity, and then the weight functions w_x, w_y and w_z are replaced by interpolation functions $\psi_m = \psi_m(x)$, $m = 1, ..., NV$. Applying this procedure for the directions x, y and z, and restricting the nodal interpolation functions to each element e, in the direction x, we have

$$\sum_e \int_{\Omega_e} \sum_{i,j\in e} \rho^e \frac{Du_j}{Dt} \psi_i^e \psi_j^e d\Omega - \sum_e \int_{\Omega_e} \sum_{i,k\in e} \frac{\partial \psi_i^e}{\partial x} P_k^e p_k d\Omega - \frac{1}{Re} \sum_e \int_{\Omega_e} \sum_{i,j\in e} \mu^e \left(\frac{\partial \psi_i^e}{\partial x}\frac{\partial \psi_j^e}{\partial x} u_j + \frac{\partial \psi_i^e}{\partial y}\frac{\partial \psi_j^e}{\partial y} u_j + \right.$$
$$\left. \frac{\partial \psi_i^e}{\partial z}\frac{\partial \psi_j^e}{\partial z} u_j + \frac{\partial \psi_i^e}{\partial x}\frac{\partial \psi_j^e}{\partial x} u_j + \frac{\partial \psi_i^e}{\partial y}\frac{\partial \psi_j^e}{\partial x} v_j + \frac{\partial \psi_i^e}{\partial z}\frac{\partial \psi_j^e}{\partial x} w_j \right) d\Omega - \frac{1}{Fr^2} \sum_e \int_{\Omega_e} \sum_{i,j\in e} \rho^e \psi_i^e \psi_j^e g_{x,j} d\Omega = 0 \tag{15}$$

In the direction y,

$$\sum_e \int_{\Omega_e} \sum_{i,j\in e} \rho^e \frac{Dv_j}{Dt} \psi_i^e \psi_j^e d\Omega - \sum_e \int_{\Omega_e} \sum_{i,k\in e} \frac{\partial \psi_i^e}{\partial y} P_k^e p_k d\Omega - \frac{1}{Re} \sum_e \int_{\Omega_e} \sum_{i,j\in e} \mu^e \left(\frac{\partial \psi_i^e}{\partial x}\frac{\partial \psi_j^e}{\partial x} v_j + \frac{\partial \psi_i^e}{\partial y}\frac{\partial \psi_j^e}{\partial y} v_j + \right.$$
$$\left. \frac{\partial \psi_i^e}{\partial z}\frac{\partial \psi_j^e}{\partial z} v_j + \frac{\partial \psi_i^e}{\partial x}\frac{\partial \psi_j^e}{\partial y} u_j + \frac{\partial \psi_i^e}{\partial y}\frac{\partial \psi_j^e}{\partial y} v_j + \frac{\partial \psi_i^e}{\partial z}\frac{\partial \psi_j^e}{\partial y} w_j \right) d\Omega - \frac{1}{Fr^2} \sum_e \int_{\Omega_e} \sum_{i,j\in e} \rho^e \psi_i^e \psi_j^e g_{y,j} d\Omega = 0 \tag{16}$$

In the direction z,

$$\sum_e \int_{\Omega_e} \sum_{i,j\in e} \rho^e \frac{Dw_j}{Dt} \psi_i^e \psi_j^e d\Omega - \sum_e \int_{\Omega_e} \sum_{i,k\in e} \frac{\partial \psi_i^e}{\partial z} P_k^e p_k d\Omega - \frac{1}{Re} \sum_e \int_{\Omega_e} \sum_{i,j\in e} \mu^e \left(\frac{\partial \psi_i^e}{\partial x}\frac{\partial \psi_j^e}{\partial x} w_j + \frac{\partial \psi_i^e}{\partial y}\frac{\partial \psi_j^e}{\partial y} w_j + \right.$$
$$\left. \frac{\partial \psi_i^e}{\partial z}\frac{\partial \psi_j^e}{\partial z} w_j + \frac{\partial \psi_i^e}{\partial x}\frac{\partial \psi_j^e}{\partial z} u_j + \frac{\partial \psi_i^e}{\partial y}\frac{\partial \psi_j^e}{\partial z} v_j + \frac{\partial \psi_i^e}{\partial z}\frac{\partial \psi_j^e}{\partial z} w_j \right) d\Omega - \frac{1}{Fr^2} \sum_e \int_{\Omega_e} \sum_{i,j\in e} \rho^e \psi_i^e \psi_j^e g_{z,j} d\Omega = 0 \tag{17}$$

The equation of continuity Eq. (2) is evaluated on the free nodes of pressure, then weight function q is approximated by the interpolation functions associated with the pressure $P_r(x)$, resulting

$$\sum_e \int_{\Omega^e} \sum_n \left(\frac{\partial \psi_n}{\partial x} u_n + \frac{\partial \psi_n}{\partial y} v_n + \frac{\partial \psi_n}{\partial z} w_n \right) P_r d\Omega = 0 \tag{18}$$

for $r = 1, \ldots, NP$. Restricting the interpolation functions to each element e, we have

$$\sum_e \int_{\Omega^e} \sum_{j,k\in e} \left(\frac{\partial \psi_j^e}{\partial x} u_j + \frac{\partial \psi_j^e}{\partial y} v_j + \frac{\partial \psi_j^e}{\partial z} w_j \right) P_k^e d\Omega = 0 \tag{19}$$

The Eq. (15), (16) e (17) can be represented in an ordinary differential equations system form

$$\mathbf{M}_{\rho,x}\frac{Du}{Dt}-\frac{1}{Re}\left((2\mathbf{K}_{xx}+\mathbf{K}_{yy}+\mathbf{K}_{zz})\mathbf{u}+\mathbf{K}_{xy}\mathbf{v}+\mathbf{K}_{xz}\mathbf{w}\right)-\mathbf{G}_x\mathbf{p}-\frac{1}{Fr^2}\mathbf{M}_{\rho,x}\mathbf{g}_x=0$$

$$\mathbf{M}_{\rho,y}\frac{Dv}{Dt}-\frac{1}{Re}\left(\mathbf{K}_{yx}\mathbf{u}+(\mathbf{K}_{xx}+2\mathbf{K}_{yy}+\mathbf{K}_{zz})\mathbf{v}+\mathbf{K}_{yz}\mathbf{w}\right)-\mathbf{G}_y\mathbf{p}-\frac{1}{Fr^2}\mathbf{M}_{\rho,y}\mathbf{g}_y=0$$

$$\mathbf{M}_{\rho,z}\frac{Dw}{Dt}-\frac{1}{Re}\left(\mathbf{K}_{zx}\mathbf{u}+\mathbf{K}_{zy}\mathbf{v}+(\mathbf{K}_{xx}+\mathbf{K}_{yy}+2\mathbf{K}_{zz})\mathbf{w}+\right)-\mathbf{G}_z\mathbf{p}-\frac{1}{Fr^2}\mathbf{M}_{\rho,z}\mathbf{g}_z=0$$

$$\mathbf{D}_x\mathbf{u}+\mathbf{D}_y\mathbf{v}+\mathbf{D}_z\mathbf{w}=0 \tag{20}$$

where $\mathbf{u}=[u_1,\ldots,u_{NV}]^T$, $\mathbf{v}=[v_1,\ldots,v_{NV}]^T$, $\mathbf{w}=[w_1,\ldots,w_{NV}]^T$ $\mathbf{p}=[p_1,\ldots,p_{NP}]^T$, $\mathbf{g}_x=[g_1^x,\ldots,g_{NV}^x]^T$, $\mathbf{g}_y=[g_1^y,\ldots,g_{NV}^y]^T$, $\mathbf{g}_z=[g_1^z,\ldots,g_{NV}^z]^T$ are the vectors of the nodal values for the velocity and pressure variables, and the gravity forces.

The dimensions of the matrices of the equations system (20) are $NV\times NP$ for $\mathbf{G}_x$, $\mathbf{G}_y$ and $\mathbf{G}_z$, $NP\times NV$ for $\mathbf{D}_x$, $\mathbf{D}_y$ e $\mathbf{D}_z$ and $NV\times NV$ for all others.

3.3 Semi-Lagrangean Method

This method was introduced in the beginning of the 80's by (Robert, 1981) and (Pironneau, 1982), and the basic idea is based on the discretization of the solution of the Lagrangean derivative in time instead of the eulerian derivative. As an example, one can consider a Semi-Lagrangean scheme of any equation of any type convection-diffusion.

The material derivative of a scalar u is given in the three-dimensional space as

$$\frac{Du}{Dt}=\frac{\partial u}{\partial t}+u\frac{\partial u}{\partial x}+v\frac{\partial u}{\partial y}+w\frac{\partial u}{\partial z} \tag{21}$$

The basic idea of the Semi-Lagrangean method is to follow a fluid particle during its path through the mesh during the flow. The method is explicit, where is necessary the information of the values of the components of velocity in the current time. Therefore, the method approximate those values in the previous step time on the path. Basically, the Semi-Lagrangean formulation is given by

$$\frac{Du}{Dt}(p)=\frac{\mathbf{u}_p^{n+1}-\mathbf{u}_{p^*}^n}{\Delta t} \tag{22}$$

where

$$p^*=p-\Delta t\mathbf{u}_p \tag{23}$$

where p is any point in the mesh and p^* defines the point p in the previous step time. The calculus of $\mathbf{u}$ in the point p^* is made by a linear interpolation between the neighbors points. This interpolations is dependent from where the point p^* is located inside the domain, such as: over an edge, over a vertex, over a face of a wedge element, inside a wedge element or outside the domain.

Then, the equations system (20) can be written as follows.

$$\mathbf{M}_{\rho,x}\left(\frac{u_p^{n+1}-u_{p^*}^n}{\Delta t}\right)-\frac{1}{Re}\left((2\mathbf{K}_{xx}+\mathbf{K}_{yy}+\mathbf{K}_{zz})\mathbf{u}+\mathbf{K}_{xy}\mathbf{v}+\mathbf{K}_{xz}\mathbf{w}\right)-\mathbf{G}_x\mathbf{p}-\frac{1}{Fr^2}\mathbf{M}_{\rho,x}\mathbf{g}_x=0$$

$$\mathbf{M}_{\rho,y}\left(\frac{v_p^{n+1}-v_{p^*}^n}{\Delta t}\right)-\frac{1}{Re}\left(\mathbf{K}_{yx}\mathbf{u}+(\mathbf{K}_{xx}+2\mathbf{K}_{yy}+\mathbf{K}_{zz})\mathbf{v}+\mathbf{K}_{yz}\mathbf{w}\right)-\mathbf{G}_y\mathbf{p}-\frac{1}{Fr^2}\mathbf{M}_{\rho,y}\mathbf{g}_y=0$$

$$\mathbf{M}_{\rho,z}\left(\frac{w_p^{n+1}-w_{p^*}^n}{\Delta t}\right)-\frac{1}{Re}\left(\mathbf{K}_{zx}\mathbf{u}+\mathbf{K}_{zy}\mathbf{v}+(\mathbf{K}_{xx}+\mathbf{K}_{yy}+2\mathbf{K}_{zz})\mathbf{w}+\right)-\mathbf{G}_z\mathbf{p}-\frac{1}{Fr^2}\mathbf{M}_{\rho,z}\mathbf{g}_z=0$$

$$\mathbf{D}_x\mathbf{u}+\mathbf{D}_y\mathbf{v}+\mathbf{D}_z\mathbf{w}=0 \tag{24}$$

4. NUMERICAL METHOD

The numerical procedure implemented to solve the conservation equations is based on the Projection method, initially proposed by (Chorin, 1968), and formalized by (Gresho, 1990)(Gresho and Sani, 1987). Thus, instead of solving one large system, we solve two smaller decoupled systems of equations, reducing the time of computation.

The Projection method based on LU decomposition is obtained though the fatoration in blocks of the resulting linear system. This suggests that the split of the velocity and pressure is made after the discretization in space and in time of the governing equations. Consider the discretized equations in time and space as follows

$$\mathbf{M}\rho\left(\frac{\mathbf{u}^{n+1}-\mathbf{u}_*^n}{\Delta t}\right)-\frac{1}{Re}\mathbf{K}\mathbf{u}^{n+1}-\mathbf{G}\mathbf{p}^{n+1}-\frac{1}{Fr^2}\mathbf{M}_\rho\mathbf{g}=0 \tag{25}$$

$$\mathbf{D}\mathbf{u}^{n+1}=0 \tag{26}$$

The Eq.(25) together with Eq.(26) compose an equation system that can be represented in the following way

$$\begin{bmatrix} \mathbf{B} & -\Delta t\mathbf{G} \\ \mathbf{D} & \mathbf{0} \end{bmatrix}\begin{bmatrix} \mathbf{u}^{n+1} \\ \mathbf{p}^{n+1} \end{bmatrix}=\begin{bmatrix} \mathbf{r}^n \\ \mathbf{0} \end{bmatrix}+\begin{bmatrix} \mathbf{bc_1} \\ \mathbf{bc_2} \end{bmatrix} \tag{27}$$

The matrix $\mathbf{B}$ is given by

$$\mathbf{B}=\mathbf{M}_\rho-\frac{\Delta t}{Re}\mathbf{K} \tag{28}$$

The right side of the equations system (27) represents the variables known in time n, added the boundary conditions, that are the contributions of the known values of velocity and pressure.

$$\mathbf{r}^n=-\Delta t\left(-\frac{1}{Fr^2}\mathbf{M}_\rho\mathbf{g}\right)+\mathbf{M}_\rho\mathbf{u}_*^n \tag{29}$$

The method consists on decomposing the equations system (27) though a block fatoration. The work of (Lee et al., 2001) presented several ways of factoring such type of matrix, where each different factoring results on a new family of methods. By using a LU canonical block factoring, we obtain the following system

$$\begin{bmatrix} \mathbf{B} & \mathbf{0} \\ \mathbf{D} & \Delta t\mathbf{D}\mathbf{B}^{-1}\mathbf{G} \end{bmatrix}\begin{bmatrix} \mathbf{I} & -\Delta t\mathbf{B}^{-1}\mathbf{G} \\ \mathbf{0} & \mathbf{I} \end{bmatrix}\begin{bmatrix} \mathbf{u}^{n+1} \\ \mathbf{p}^{n+1} \end{bmatrix}=\begin{bmatrix} \mathbf{r}^n \\ \mathbf{0} \end{bmatrix}+\begin{bmatrix} \mathbf{bc_1} \\ \mathbf{bc_2} \end{bmatrix} \tag{30}$$

The system as given in (30), if solved, results on the method known as Uzawa method (Chang et all., 2002). However, this method have an high computational cost, because of the need of inversion of the matrix $\mathbf{B}$ at each iteration. In this case, we used a process of approximations called Lumping for the inverse of the matrix $\mathbf{B}$. The new matrix is a diagonal matrix defined as the sum of the values of each line from the original matrix, storing the sum in the position of the element on the diagonal. Therefore, we have

$$\mathbf{B}\widetilde{\mathbf{u}}=\mathbf{r}^n+\mathbf{bc}_1 \tag{31}$$

$$\Delta t\mathbf{D}\mathbf{M}_\rho^{-1}\mathbf{G}\mathbf{p}^{n+1}=-\mathbf{D}\widetilde{\mathbf{u}}+\mathbf{bc}_2 \tag{32}$$

$$\mathbf{u}^{n+1}=\widetilde{\mathbf{u}}+\Delta t\mathbf{M}_\rho^{-1}\mathbf{G}\mathbf{p}^{n+1} \tag{33}$$

A procedure for the solution of the equations is given in the following order:

- Evaluate $\widetilde{\mathbf{u}}$ from Eq. (31);
- Evaluate $\mathbf{p}^{n+1}$ from Eq. (32);
- Evaluate the final velocity $\mathbf{u}^{n+1}$ using Eq. (33);
- Update the time step and continue until the final time or convergence are reached.

After update the components of the final velocity u^{n+1} and v^{n+1}, is necessary to update the component of the velocity w by using the equation of continuity, guaranteeing the condition of incompressibility.

5. NUMERICAL RESULTS

The method was validated for the case of stationary incompressible flow, producing nodal values close to the exact values. A solution that can be compared with the resulting solution of the simulations is the exact solution of the Poisson equation. The solution matches the corresponding velocity component in direction x of a stationary and developed flow over a square open duct with height $H = \frac{L}{2}$, i.e., the half of width $a = L$, considering that the surface is a symmetry line. The exact solution is given by

$$u(y,z) = \frac{(1-y^2)}{2} - \frac{16}{\pi^3} \sum_{k=1,k\ odd}^{\infty} \left\{ \frac{sin\left(k\pi\left(1+y\right)/2\right)}{k^3 sinh\left(k\pi\right)} \times \left(sinh\left(k\pi\left(1+z\right)/2\right) + sinh\left(k\pi\left(1-z\right)/2\right)\right) \right\} \quad (34)$$

A square domain LxL for the surface, where $L = 2\ m$ was defined. In this case, no-slip conditions were imposed on the wall of the domain for the velocity components u, v and w. The pressure has zero value on the outflow of the duct. The velocity component in direction z has zero value in the upper and lower levels of the domain. The condition for fully developed flow defined at the inflow of the duct is given by the Eq. (34). The geometry of the domain is presented in the Figure 1(a), which shows the dimensions of the sides of the duct and the inflow of fluid.

When the stationary state is achieved, the values of the components of velocities along the duct are the same that those defined in the inflow of the duct. Then, one can compare the numerical results with the exact solution given by the Eq. (34). The model for this flow is detailed as follow. Dimension of domain: $2.0\ m$ x $2.0\ m$ x $1.0\ m$; Width of inflow: $2.0\ m$; Viscosity: $1.00\ Ns/m^2$; Density $1.0\ kg/m^3$; Mesh 1: 15x15x6 points, total of elements: 1960; Mesh 2: 21x21x6 points, total of elements: 4000, both equally distributed into five layers of elements, and Reynolds number: 10;

The Figure 1(b) shows the numerical result obtained by the simulation. The considered region when comparing the numerical result with the exact solution for this case is the outflow of the duct. From the figure, it can be seen that the more refined the mesh is, the more accurate the method is.

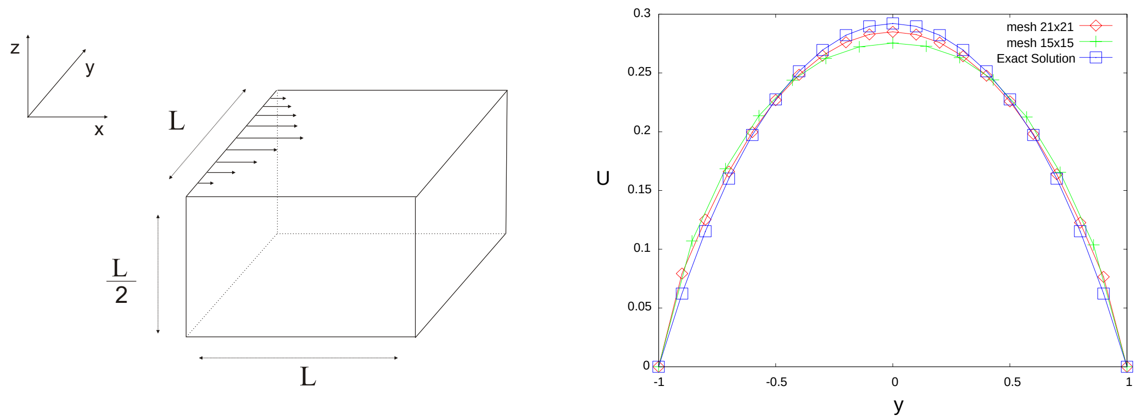

(a) (b)

Figure 1. a) Domain geometry. b) Comparison of obtained results with exact solution.

The problem of backward-step was used to illustrate the features of the developed method. This case presents a high complexity factor, because of the developing of the boundary layer and the cyclical flow zone.

The geometry of the problem is shown in Figure 2(a). The numerical simulation was made by using as initial conditions $u = 1.0\ m/s$, $v = 0\ m/s$ and $w = 0\ m/s$. In the simulation, a total of 12400 wedge elements were used, equally distributed into five layers of elements. The results were obtained in the second layer of the domain and at the outflow of the duct.

The physical parameters and the flow features used are detailed as follow. Dimension of the domain: $3.0\ m$ x $1.0\ m$ x $1.0\ m$; Width of inflow: $0.5\ m$; Viscosity : $1.00\ Ns/m^2$; Density : $1.0\ kg/m^3$; Scale: $L = 1.0\ m$ and $H = 1.0\ m$ and Reynolds number : $10, 100$ e 1000.

In this case were applied no-slip conditions on the walls of the domain for the velocity components u,v and w. This means that the values of velocities are zero and the boundary condition for pressure is of Neumann type. The pressure values are zero at the end of the duct.

Figure 2(b) shows one layer example of the mesh formed by wedge elements, indicating the first wedge element. In the figure, the dots indicate the existence of other elements to form the entire mesh. Each layer can have different height size but the same number of elements among others.

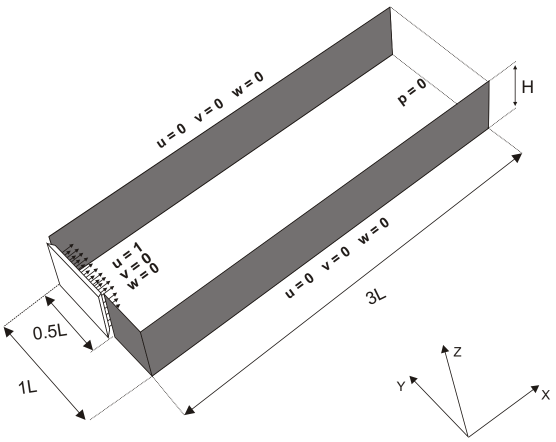

(a)

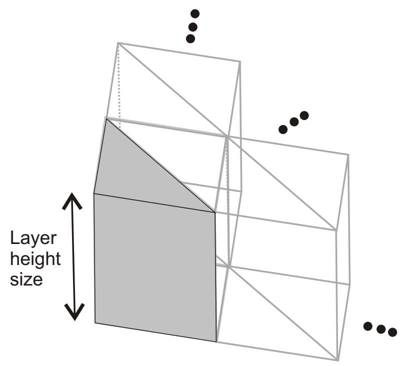

(b)

Figure 2. a) Geometry e boundary conditions. b) One layer example of the mesh formed by wedges.

Figure 3 shows a graph in log scale which shows the number of iterations and the residue obtained from the conjugate gradient method used on the solution of the linear equation systems resulted from the discretization of Navier–Stokes equations. The number of iterations needed for the conjugate gradient residue became close enough to zero indicates the velocity that the method reaches a stationary state.

The results showed in Figures 4, 5 and 6 represent data extracted in three different stages during the same simulation. The first column represents the first stage, where data were extracted after two iterations of the method. The second column represents the intermediate stage, where data were extracted after twenty iterations. The third column represents the last stage, where data were extracted when the simulation reaches a stationery state.

In the simulation showed by Figure 4, the Reynolds number is considered low $Re = 10$. The viscous terms of Navier-Stokes equations have more influence over the convective terms on the fluid flow. In this case the flow expand right after the obstacle. The boundary layer of the velocity component in direction x has low gradient and then it becomes thick, as can be seen in the figure.

In the simulations showed in Figures 5 e 6, we can see a fluid flow with low viscosity. The high value of Reynolds number reduces the influence of the viscous term and we can notice negative values in the component of direction x of the velocity, where the step is located. This behavior indicates the formation of recycling on the flow as expected. It is also verified that depending of the Reynolds number used, the width of the recycling region raises. This fact can be observed in the Figure 8 which shows the fluid flow vector field for the three cases simulated.

Figure 7 shows the simulation of the velocity component in direction x, containing all the domain levels. We can observe the behavior of the fluid flow at the inflow of the model under different Reynolds number.

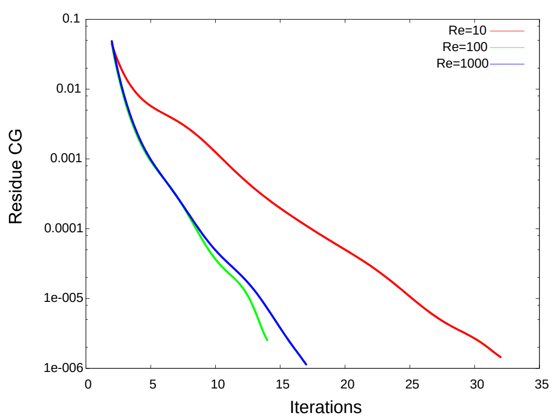

Figure 3. Graph in log scale of the residue of the conjugate gradient method over iterations varying the Reynolds number.

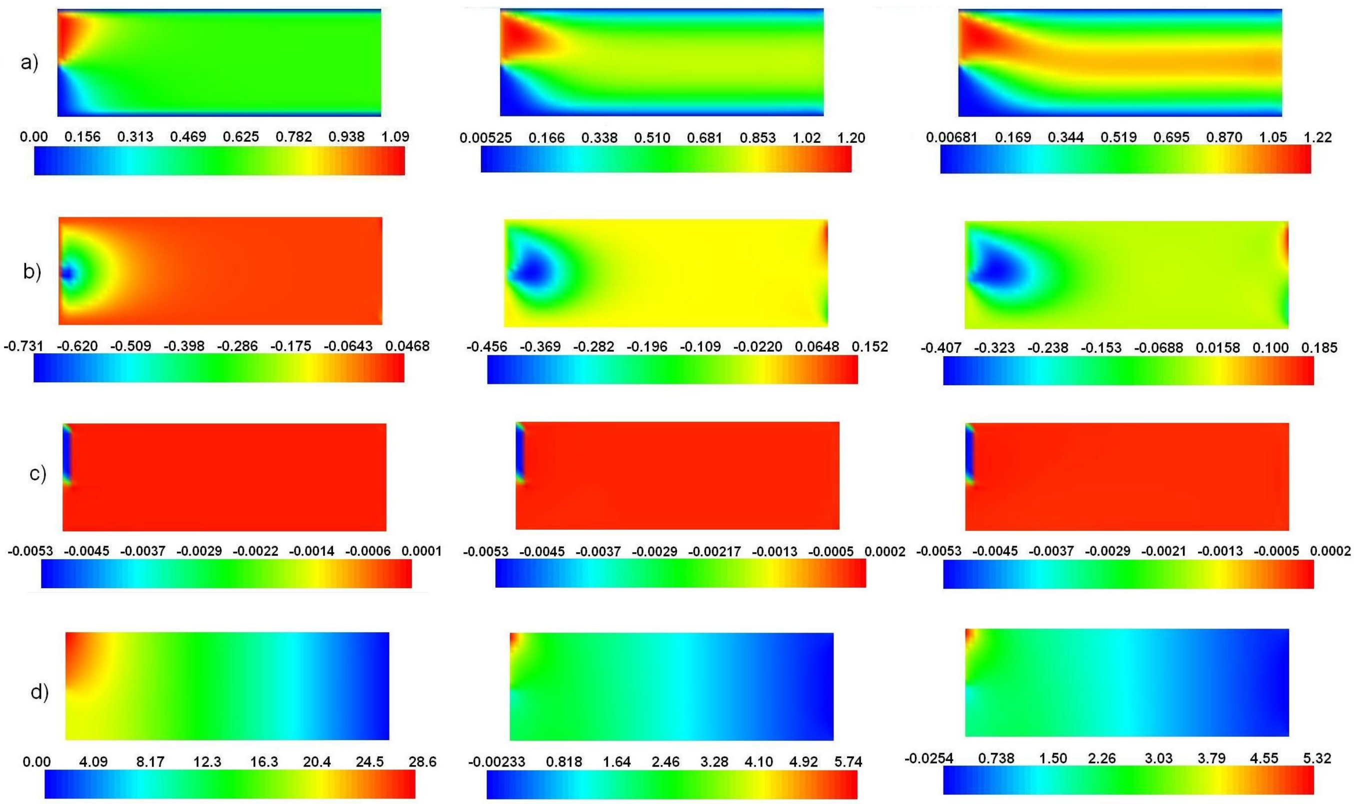

Figure 4. Simulation using $Re = 10$, a) evolution of the velocity component in direction x, b) y, c) z and d) pressure

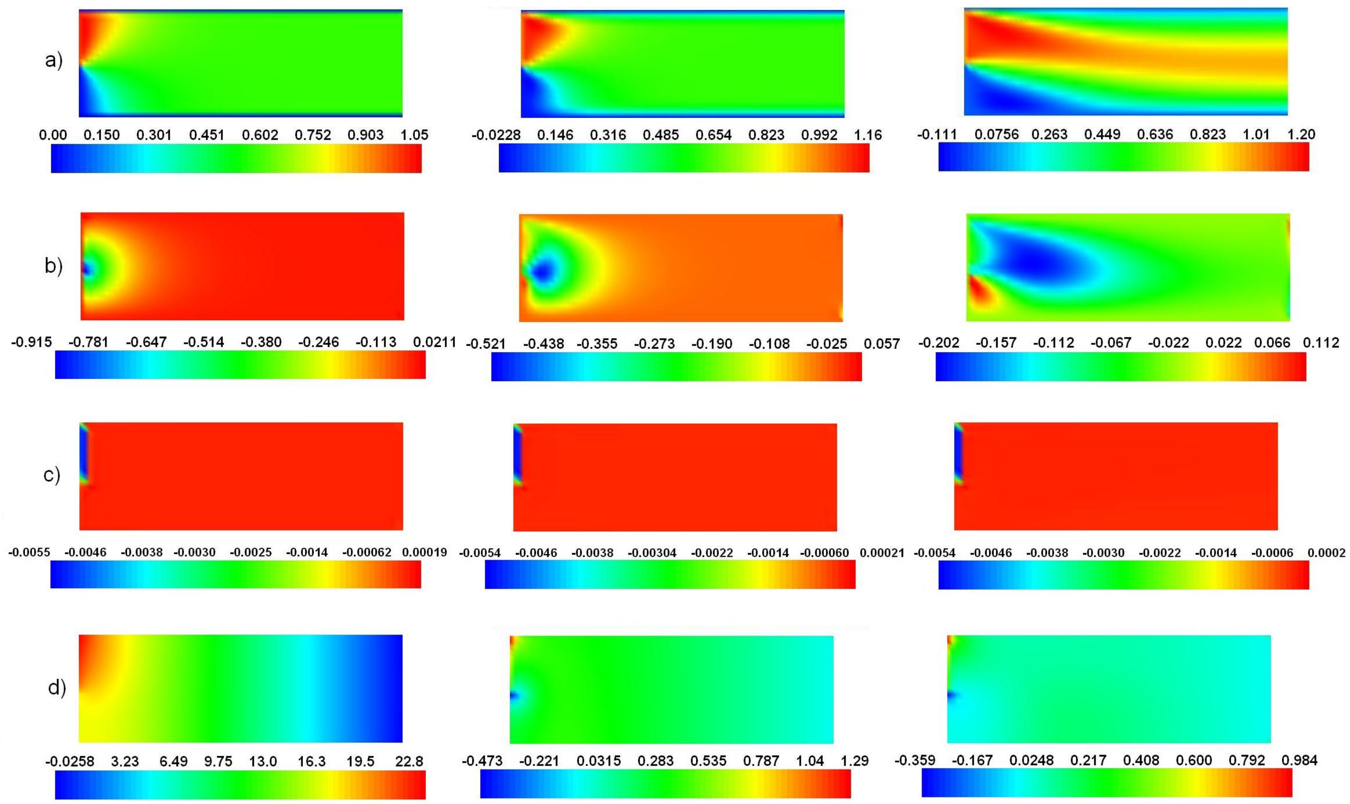

Figure 5. Simulation using $Re = 100$, a) evolution of the velocity component in direction x, b) y, c) z and d) pressure

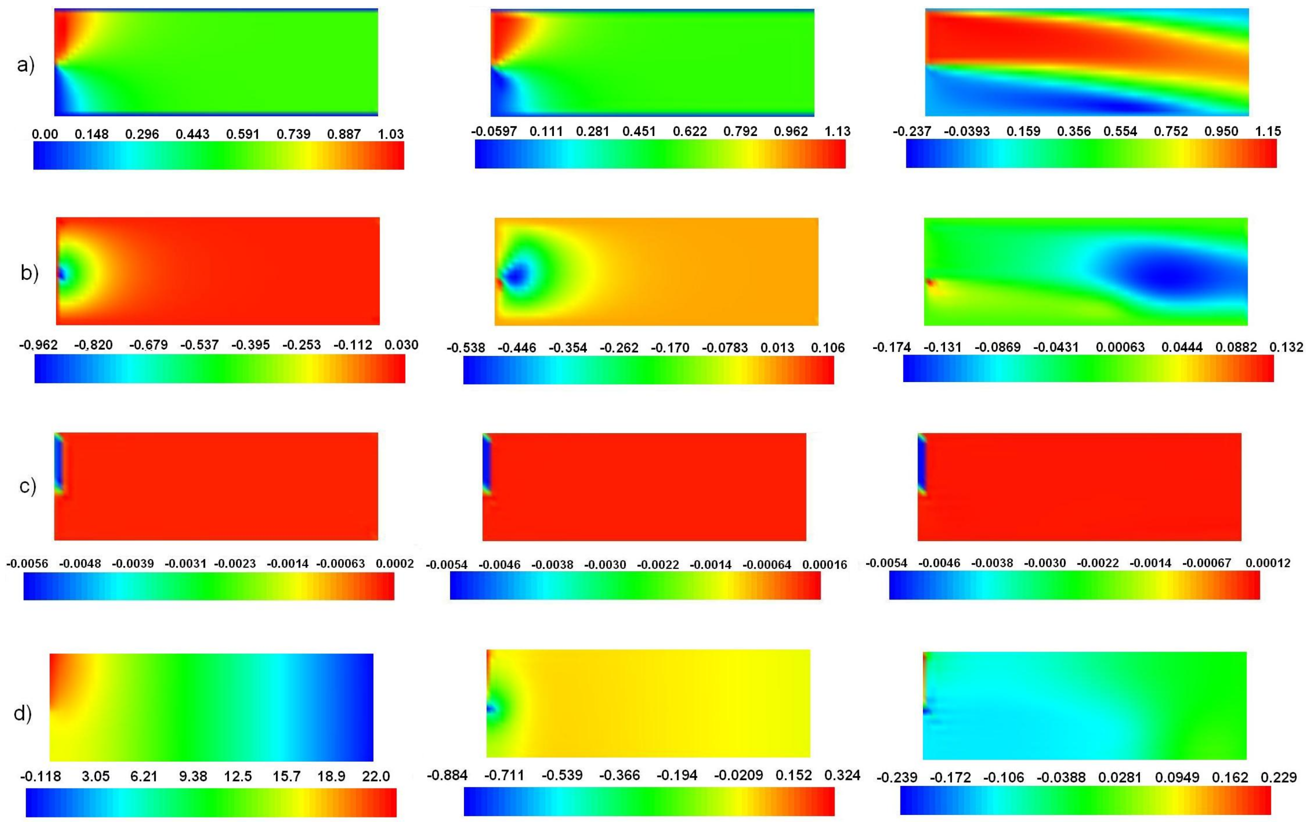

Figure 6. Simulation using $Re = 1000$, a) evolution of the velocity component in direction x, b) y, c) z and d) pressure

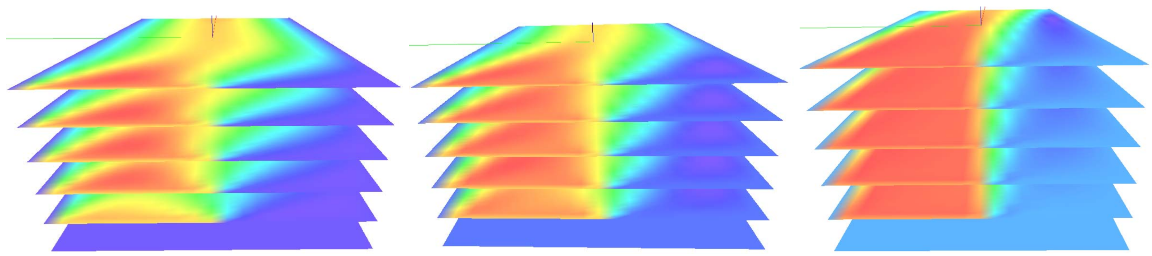

(a) (b) (c)

Figure 7. Numerical simulations of the fluid flow in the backward-step in a point of view at the inflow of the duct, velocity component fild in direction x a) $Re = 10$, b) $Re = 100$ e c) $Re = 1000$.

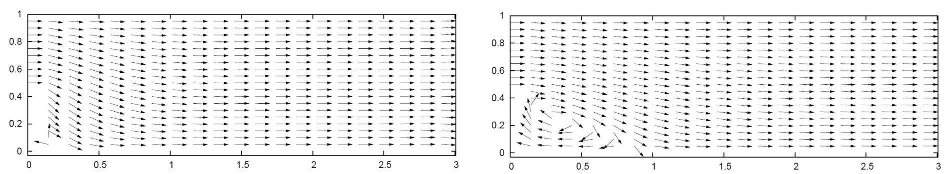

(a) (b)

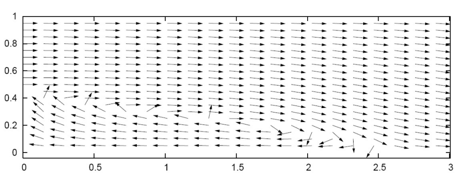

(c)

Figure 8. Vector fields of fluid flow, (a) $Re = 10$, (b) $Re = 100$ and (c) $Re = 1000$

6. CONCLUSION

The goal of this work was the mathematical modeling and development of a method for the simulation of fluid flows in three-dimensional domains. The finite elements method was used to discretize the equations. The Projection method based on LU decomposition was used to extract the pressure component, and the using of Lumped matrices reduced the complexity of the algorithms, where the pressure gradient were calculated independently at each iteration. Then, the velocity value were corrected by the continuity equation, keeping the divergence field null. The solution of the linear systems was obtained by using the conjugate gradient method.

Future works about validation of the 3D simulation involve comparing the achieved results to real measurements obtained in controlled experiments and seeking similar works in this field that complement the analysis of the simulation itself.

7. ACKNOWLEDGEMENTS

The authors acknowledges the Brazilian agencies FAPESP (grant 04/12764-6), Furnas Centrais Elétricas S.A. for the financial support.

8. REFERENCES

Anderson, J. D., 1995, "Computational Fluid Dynamics", McGraw-Hill - N.Y.

Batchelor, G. K., 1970, "An Introduction to Fluid Dynamics", Cambridge.

Becker, E. B., Carey, G. F., and Oden, J. T., 1981, "Finite Elements An Introduction", Dover.

Chorin, A. J., 1968, "Numerical solution of the Navier-Stokes equations", Mathematics of Computation, Vol.22, pp. 745-762.

Chung, T. J., 1978, "Finite element analysis in fluid dynamics", McGraw- Hill, New York, 378p.

Ferziger, J. H. and Períc, M., 1999, "Computational Methods for Fluid Dynamics", Heidelberg, Springer-Verlag.

Flecther, C. A., 1992, "Computational Techniques for Fluid Flows", Heidelberg, Springer-Verlag.

Fortuna, A. O., 2000, "Técnicas Computacionais para Dinâmica dos Fluidos", Edusp.

Gresho P., 1990, "On the theory of semi-implicit projection methods for viscous incompressible flow and its implementation via the finite element method that also introduces a nearly consistent mass matrix. Part 1: theory. Part 2: implementation.", International Journal for Numerical Methods in Fluids, Vol.11, pp. 587-659.

Gresho P, Sani R., 1987, "On pressure boundary conditions for the incompressible Navier-Stokes equations.", International Journal for Numerical Methods in Fluids, Vol.7, pp. 1111-1145.

Lee, M. J., Oh, B. D., and Kim, Y. B., 2001, " Canonical fractionalstep methods and consistent boundary conditions for the incompressible Navier-Stokes equations", Journal of Computational Physics, Vol. 168, pp. 73-100.

Maliska, C. A. , 1995, " Transferência de Calor e Mecânica dos Fluidos Computacional", LTC Editora - Rio de Janeiro.

Robert, A., 1981, "A stable numerical integration scheme for the primitive meteorologica equations", Atmos. Ocean, pp. 19-35.

Panton, R. L., 1984, "Incompressible flow", John Wiley and Sons.

Peyret, R. and Taylor, T. D., 1983, " Computational Methods for Fluid Flow", Springer-Verlag.

Pironneau, O., 1982, "On the transpor-diffusion algorithm and its applications to the Navier-Stokes equation", Numer Math, pp. 38-309.

Chang, W., Giraldo, F., and Perot, B., 2002, "Analysis of an exact fractional step method", Journal of Computational Physics, Vol. 180, pp. 180-183.

Zienkiewicz, O. C. and Taylor, R. L., 2000, "The Finite Element Method Volume 1: The Basis", Wiley John and Sons, 5th edition.

Zienkiewicz, O. C. and Cheung, Y. K., 1965, "Finite elements in the solution of field problems", The Engineer, 507-10 edition.

9. Responsibility notice

The authors are the only responsible for the printed material included in this paper.